

# Degradation of ribosomal and chaperone proteins is attenuated during the differentiation of replicatively aged C2C12 myoblasts

Alexander D. Brown , Claire E. Stewart\*  & Jatin G. Burniston\* 

Research Institute for Sport & Exercise Sciences, Liverpool John Moores University, Liverpool, UK

## Abstract

**Background** Cell assays are important for investigating the mechanisms of ageing, including losses in protein homeostasis and ‘proteostasis collapse’. We used novel isotopic labelling and proteomic methods to investigate protein turnover in replicatively aged (>140 population doublings) murine C2C12 myoblasts that exhibit impaired differentiation and serve as a model for age-related declines in muscle homeostasis.

**Methods** The Absolute Dynamic Profiling Technique for Proteomics (Proteo-ADPT) was used to investigate proteostasis in young (passage 6–10) and replicatively aged (passage 48–50) C2C12 myoblast cultures supplemented with deuterium oxide (D<sub>2</sub>O) during early (0–24 h) or late (72–96 h) periods of differentiation. Peptide mass spectrometry was used to quantify the absolute rates of abundance change, synthesis and degradation of individual proteins.

**Results** Young cells exhibited a consistent ~25% rise in protein accretion over the 96-h experimental period. In aged cells, protein accretion increased by 32% ( $P < 0.05$ ) during early differentiation, but then fell back to baseline levels by 96-h. Proteo-ADPT encompassed 116 proteins and 74 proteins exhibited significantly ( $P < 0.05$ , FDR < 5% interaction between age  $\times$  differentiation stage) different changes in abundance between young and aged cells at early and later periods of differentiation, including proteins associated with translation, glycolysis, cell–cell adhesion, ribosomal biogenesis, and the regulation of cell shape. During early differentiation, heat shock and ribosomal protein abundances increased in aged cells due to suppressed degradation rather than heightened synthesis. For instance, HS90A increased at a rate of  $10.62 \pm 1.60$  ng/well/h in aged which was significantly greater than the rate of accretion ( $1.86 \pm 0.49$  ng/well/h) in young cells. HS90A synthesis was similar in young ( $21.23 \pm 3.40$  ng/well/h) and aged ( $23.69 \pm 1.13$  ng/well/h), but HS90A degradation was significantly ( $P = 0.05$ ) greater in young ( $19.37 \pm 2.93$  ng/well/h) versus aged ( $13.06 \pm 0.76$  ng/well/h) cells. During later differentiation the HS90A degradation ( $8.94 \pm 0.38$  ng/well/h) and synthesis ( $7.89 \pm 1.28$  ng/well/h) declined and were significantly less than the positive net balance between synthesis and degradation (synthesis =  $28.14 \pm 3.70$  ng/well/h vs. degradation =  $21.49 \pm 3.13$  ng/well/h) in young cells.

**Conclusions** Our results suggest a loss of proteome quality as a precursor to the lack of fusion of aged myoblasts. The quality of key chaperone proteins, including HS90A, HS90B and HSP7C was reduced in aged cells and may account for the disruption to cell signalling required for the later stages of differentiation and fusion.

**Keywords** Ageing; Deuterium oxide; Heavy water; Muscle regeneration; Myoblast differentiation; Protein degradation; Protein synthesis; Proteomics; Proteostasis

Received: 18 January 2022; Revised: 12 April 2022; Accepted: 12 May 2022

\*Correspondence to: Claire E. Stewart and Jatin G. Burniston, Research Institute for Sport & Exercise Sciences (RISES), Liverpool John Moores University, Tom Reilly Building, Byrom Street, Liverpool L3 3AF, UK. Email: c.e.stewart@ljmu.ac.uk; j.burniston@ljmu.ac.uk

## Introduction

Skeletal muscle is the most abundant tissue in young healthy adults and serves as a repository of amino acids that can be used to repair other tissues. Losses in muscle mass, whether due to ageing, disease, disuse atrophy or damage, negatively impact health, disease prognoses and the individual's ability to enjoy an independent life. Muscle consists of terminally differentiated myofibres that undergo atrophy or hypertrophy in response to decreases or increases in mechanical load, and regenerate in response to injury or damage through a process of satellite cell activation.<sup>1</sup> Muscle regeneration requires myoblasts to undergo differentiation and fuse to form myotubes *in vitro* or myofibres *in vivo*. The capability of muscle to regenerate declines with advancing age<sup>2,3</sup> underpinned by factors that are intrinsic to satellite cells as well as age-related changes in cell environment.<sup>4</sup> Myogenic precursor cells extracted from the muscle of 32-month-old rats exhibit impaired differentiation compared with those extracted from 3-month-old rats.<sup>5</sup> Similarly, myoblasts generated from the muscle of older humans exhibit compromised fusion,<sup>6</sup> and in addition to age-related decreases in satellite cell number,<sup>3</sup> may contribute to declines in myogenic regenerative capacity and the fibro-adipogenic phenotype of aged muscle.

Muscles of older humans can exhibit disproportionate losses of fast-twitch Type II fibres, whilst resistance exercise training may selectively reverse these effects.<sup>3</sup> This interaction between ageing and physical activity presents challenges to studies on satellite cell dysfunction and age-related muscle loss *in vivo*. Therefore models of muscle ageing *in vitro* have been generated, including serial passaging (i.e. replicative ageing), which results in a robust retardation of the myogenic programme in human muscle precursor cells.<sup>7,8</sup> Similarly, murine C2C12 myoblasts that have undergone replicative ageing *in vitro* exhibit lesser expression of the myogenic regulator factors (MRF), myogenin and myoblast determination protein 1 (MyoD)<sup>9,10</sup> and impairments in myoblast differentiation and fusion.<sup>9–11</sup> These hallmarks of muscle ageing *in vitro* also occur in muscle cells upon silencing of the progeroid gene, mitotic checkpoint serine/threonine-protein kinase (BubR1).<sup>12</sup> The mechanisms that link the loss of differentiation and lack of fusion of replicatively aged myoblasts with differences in the expression of MRF are unknown but could include deficits in proteostasis. C2C12 myoblasts exhibit high levels of protein turnover and are enriched with chaperone proteins and ribosomal protein subunits during early differentiation.<sup>13</sup> Conversely, ribosomal subunits and proteins involved in proteostasis become significantly less abundant in the muscle of older adults<sup>14</sup> and a collapse of proteostasis is an acknowledged component of skeletal muscle ageing.<sup>15</sup> Therefore, we hypothesized that replicatively aged myoblasts exhibit disruptions to proteostasis and the normal turnover of proteins evident in young cells, which culminates in impaired fusion.

Protein degradation is the crucial cellular process that removes damaged or misfolded proteins and, thereby, helps to prevent proteostasis collapse and the accumulation of protein aggregates that may become toxic to the cell.<sup>16</sup> Stimulation of the ubiquitin proteasome system (UPS) can extend lifespan in *C. elegans*<sup>17</sup> but few studies have specifically investigated changes to the balance between protein synthesis and protein degradation that, together, constitute protein turnover. Proteomic analysis of biosynthetically labelled samples can provide measurements of both the abundance and synthesis rate of individual proteins.<sup>18</sup> Early work,<sup>19</sup> employing radio-labelling of heat-shocked U937 pro-monocytic, human myeloid leukaemia cell line reported increases in the abundance of the heat shock proteins were accounted for by the increases in protein-specific synthesis rates. More recently, stable isotope labelling of amino acids in culture (SILAC) has been used to study the relative contributions of synthetic and degradative processes to changes in protein abundance.<sup>20</sup> Similarly, we have conducted proteomic analysis of deuterium oxide-labelled murine C2C12 muscle cells to report protein abundance and synthesis data in mole and absolute (ng) units, which benefits the biological interpretation of protein turnover data.<sup>13</sup> Our Absolute Dynamic Profiling Technique for Proteomics (Proteo-ADPT) measures protein abundance at different time points to calculate the absolute rate of abundance change, which is driven by changes to the absolute synthesis rates (ASR) and/or the absolute degradation rates (ADR) on a protein-by-protein basis.<sup>21</sup> Changes in protein abundance that are not matched by equivalent changes to the synthetic rate of the protein may be attributed to protein degradation. In the current work we have applied Proteo-ADPT to study the contributions of protein synthesis and degradation to changes in protein abundance in replicatively aged murine C2C12 cells that exhibit impaired differentiation and fail to form myotubes.

## Methods

Cell culture experiments were performed according to our previous studies<sup>9,11</sup> using young (low passage 6–10) and replicatively aged (high passage 48–50) C2C12 murine myoblasts. The protocol was designed to investigate the impact of age on early (0–24 h) or late (72–96 h) periods of differentiation. Isotopic labelling of newly synthesized proteins was achieved by supplementing media with 4% deuterium oxide (D<sub>2</sub>O; Figure 1), as described previously.<sup>13</sup> Early differentiation (ED) was investigated by culturing myoblasts (seeded at 100 000 cells/mL) in differentiation media (DM: DMEM, 2% heat-inactivated horse serum, 2 mM L-glutamine, 1% penicillin–streptomycin) supplemented with or without D<sub>2</sub>O over a period of 0–24 h. Late differentiation was investigated by first culturing myoblasts in DM for 72 h, after which myo-

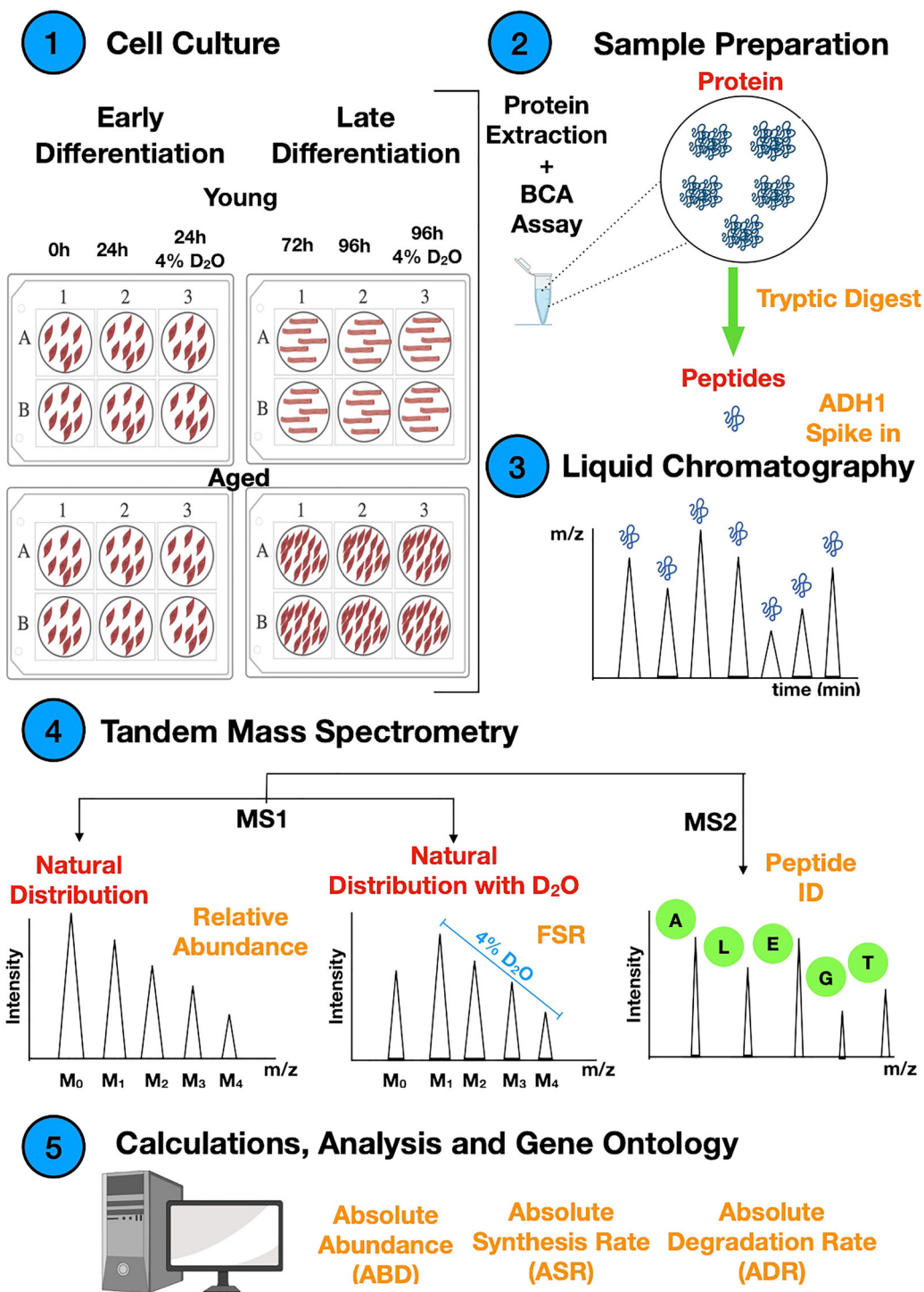


**Figure 1** Proteo-ADPT analysis young and replicatively aged myoblast differentiation. Young and aged C2C12 myoblasts were cultured in the absence or presence of D<sub>2</sub>O during either early or later periods of differentiation. Total protein was extracted and quantified and proteins were digested into peptides using trypsin. Peptide digests were spiked with 50 fmol of yeast alcohol dehydrogenase-1 (ADH1) and separated by reverse-phase ultra-performance liquid chromatography. Tandem mass spectrometry was used to record MS1 and MS2 mass spectra. MS1 peptide ion mass spectra were used to measure the relative abundance and D<sub>2</sub>O incorporation based on relative distribution of peptide mass isotopomers. The incorporation of deuterium-labelled amino acids in to newly synthesized protein causes a shift in distribution of m<sub>1</sub>, m<sub>2</sub>, m<sub>3</sub>, m<sub>4</sub> ... isotopomers, and the m<sub>0</sub> mass isotopomer declines as a function of protein synthesis. MS2 fragment ion mass spectra of each peptide were used to identify peptides against the UniProt knowledge database. The absolute dynamic profiling technique for proteomics (Proteo-ADPT) was used to calculate protein-specific synthesis, abundance and degradation data in absolute (ng) units.

tubes were transferred to fresh DM supplemented with or without D<sub>2</sub>O and cultured for a further 24 h (72–96 h of differentiation). Each differentiation period (two time points) was conducted in triplicate on one 6-well plate and in total, 12 plates ( $n = 24$  samples) were studied. Cells were extracted after being cultured in the absence or presence of D<sub>2</sub>O at 0, 24, 72, and 96 h and were processed according to our recent similar studies.<sup>13,21</sup> Cell imaging and morphological analyses (Supporting Information, Figure S1) were performed prior to DM aspiration and cells were lysed in RIPA buffer (Sigma-Aldrich, Poole, UK) including Complete™ protease inhibitors (Roche; Basel, Switzerland). Lysates were digested with sequencing grade trypsin (Promega; Madison, WI, USA) at an enzyme to protein ratio of 1:50 and aliquots were desalted using C<sub>18</sub> Zip-tips (Millipore, Billerica, MA, USA) before being dried by vacuum centrifugation and then resuspended in 0.1% formic acid spiked with 10 fmol/μL yeast ADH1 (Waters Corp. Milford, MA).

Peptide mixtures were analysed by nanoscale reverse-phase ultra-performance liquid chromatography (NanoAcquity; Waters Corp.) and online electrospray ionization quadrupole time-of-flight mass spectrometry (QToF Premier; Waters Corp.) as described in Stansfield *et al.*<sup>13</sup> Mass spectrometry data were analysed using Progenesis Quantitative Informatics for Proteomics (QI-P; Nonlinear Dynamics, Newcastle, UK) consistent with our previous work.<sup>21</sup> Log transformed MS data (peptide abundance) was normalized by inter sample abundance ratio. MS/MS spectra in Mascot generic format were searched using a locally employed Mascot server ([www.matrixscience.com](http://www.matrixscience.com); version 2.2.03) against the Swiss-Prot database restricted to 'mus musculus' which encompassed 17 006 sequences. The enzyme specificity was trypsin allowing for one missed cleavage, carbamidomethyl modification of cysteine (fixed), oxidation of methionine (variable) and deamidation of asparagine and glutamine (variable).

The fractional synthesis rates (FSR) of proteins was calculated in young and aged myoblasts at early and later stages of differentiation using methods that have been described in detail in our previous publications.<sup>21</sup> Briefly, the incorporation of deuterium into newly synthesized proteins causes a decrease in molar fraction of the monoisotopic peak and the rate constant for the decay of the molar fraction of the monoisotopic peak was calculated by a first-order exponential spanning from the start to the end of each 24 h D<sub>2</sub>O labelling period. The calculation of FSR from the rate constant depends on the number of <sup>2</sup>H exchangeable H–C bonds. This was calculated by referencing each peptide sequence against standard tables.<sup>21</sup> The FSR of each peptide was derived by dividing the rate constant by the molar percent enrichment of deuterium in the precursor pool and the total number of exchangeable H–C bonds in each peptide. Relative peptide abundance and FSR were converted to absolute values calculated from the total protein content of each well and protein

abundances normalized to the spiked-in yeast alcohol dehydrogenase standard. The rate of protein abundance change was calculated by quantifying the difference in absolute protein abundance between the end and beginning of the labelling period. The absolute degradation rate (ADR) was calculated by quantifying the difference between the ASR and rate of protein abundance change (ABR).

Data are presented as mean ± standard error of the mean (SEM) unless otherwise stated. All statistical analyses were conducted in R (version 4.0.2). Differences between age (young vs. aged) and differentiation period (early vs. late) were analysed by two-way ANOVA. Statistical significance was accepted at  $P < 0.05$  and  $q$ -values were used to calculate false discovery rate.

## Results

In young cells, differentiation was associated with a consistent rise in protein content from  $463 \pm 10$  ng/well at 0 h to  $618 \pm 65$  ng/well (~25% increase;  $P = 0.052$ ) after 96 h of differentiation. In contrast, aged cells exhibited a robust 32% increase (from  $388 \pm 40$  ng/well to  $573 \pm 63$  ng/well;  $P = 0.007$ ) in protein content during early differentiation but the protein content of aged cells then declined back to baseline levels during the later period of differentiation ( $392 \pm 43$  ng/well at 72 h and  $377 \pm 38$  ng/well at 96 h; Figure 2A). Irrespective of age, mixed protein FSR was significantly greater during early compared with late differentiation. However, the extent of the decline in mixed protein FSR between early and late periods of differentiation was significantly greater in aged cells ( $P < 0.05$  interaction between differentiation period and cell age; Figure 2C).

Proteomic analyses encompassed 611 proteotypic peptides belonging to a total of 116 individual proteins that were detected in all ( $n = 24$ ) samples. The top-ranked biological processes (Fisher  $P < 0.001$ ; Figure 2B) amongst the proteins studied, included: translation, glycolysis, cell–cell adhesion, ribosomal biogenesis and regulation of cell shape. The majority (63%; 74/116) of proteins analysed exhibited significant ( $P \leq 0.05$  and a false discovery rate of 5%) interactions in the rate of abundance change (ABR; ng/well/h) between age and stage of differentiation (Figure 3). In young cells, protein accretion was consistent and most individual proteins exhibited positive ABR values that were similar during early and late periods of differentiation. In aged cells 54 proteins exhibited positive ABR values that were greater than those of young myoblasts during early differentiation. In most cases the abundance of these proteins had been significantly less in aged cells at the 0 h timepoint (Figure 3A), therefore, the greater ABR compensated for the lower starting abundance and brought the proteome profile of aged cells more closely in line with that of young myoblasts at the end of the early

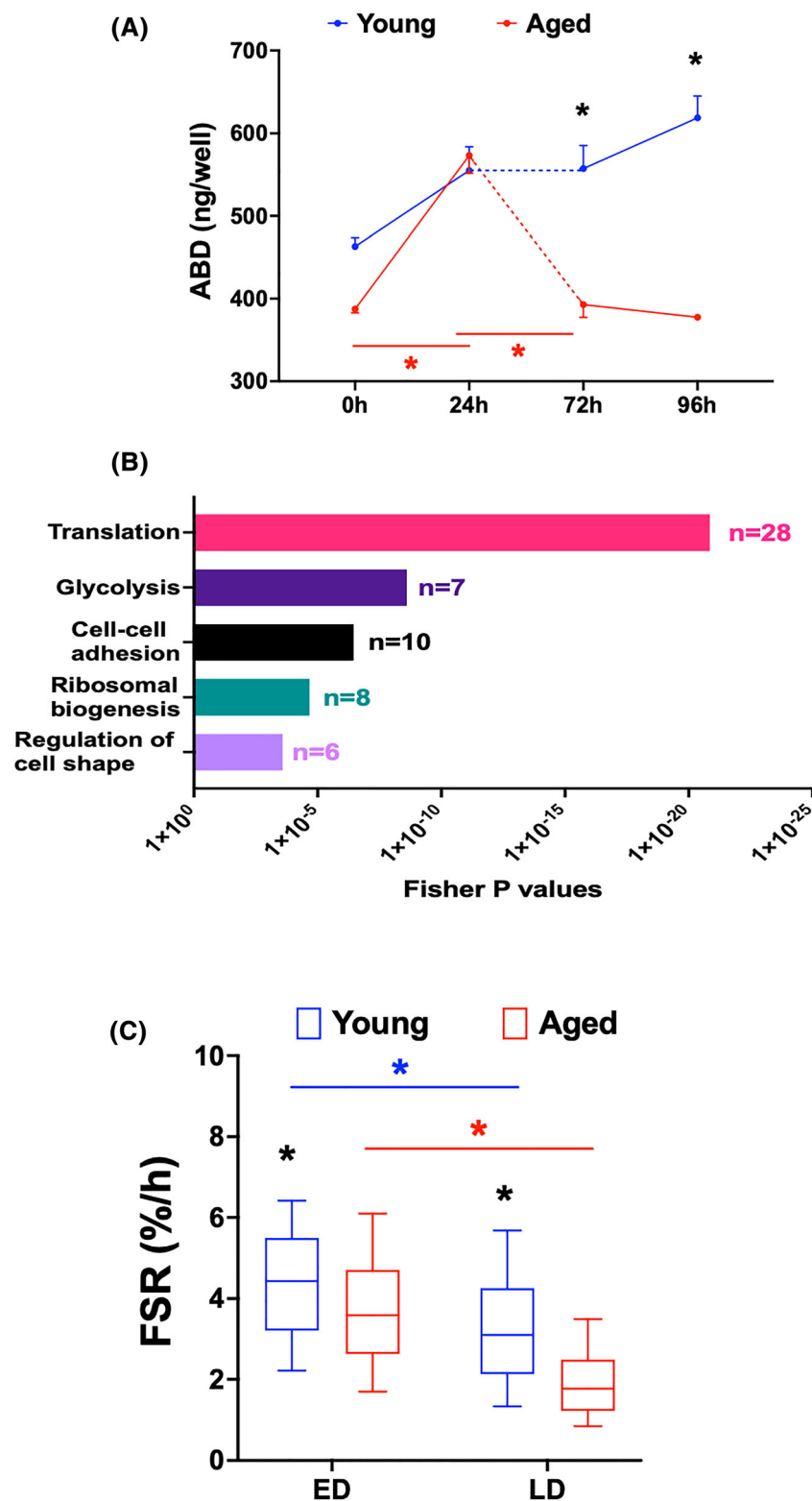


**Figure 2** Myotube formation is impaired in replicatively aged C2C12 myoblasts. (A) Absolute abundance in young versus aged myoblasts at 0, 24, 72, and 96 h. (B) Gene ontology group for biological processes in 116 proteins matched for abundance, synthesis and degradation. Fisher extract p values quantified using David GO. (C) Fractional synthesis rates of young and aged myoblasts at early differentiation and late differentiation. Abundance data presented as mean  $\pm$  SEM and FSR data presented as median and interquartile range. Significance (\*) between young and aged was set at  $P < 0.05$ . All experiments  $N = 3$  in duplicate.



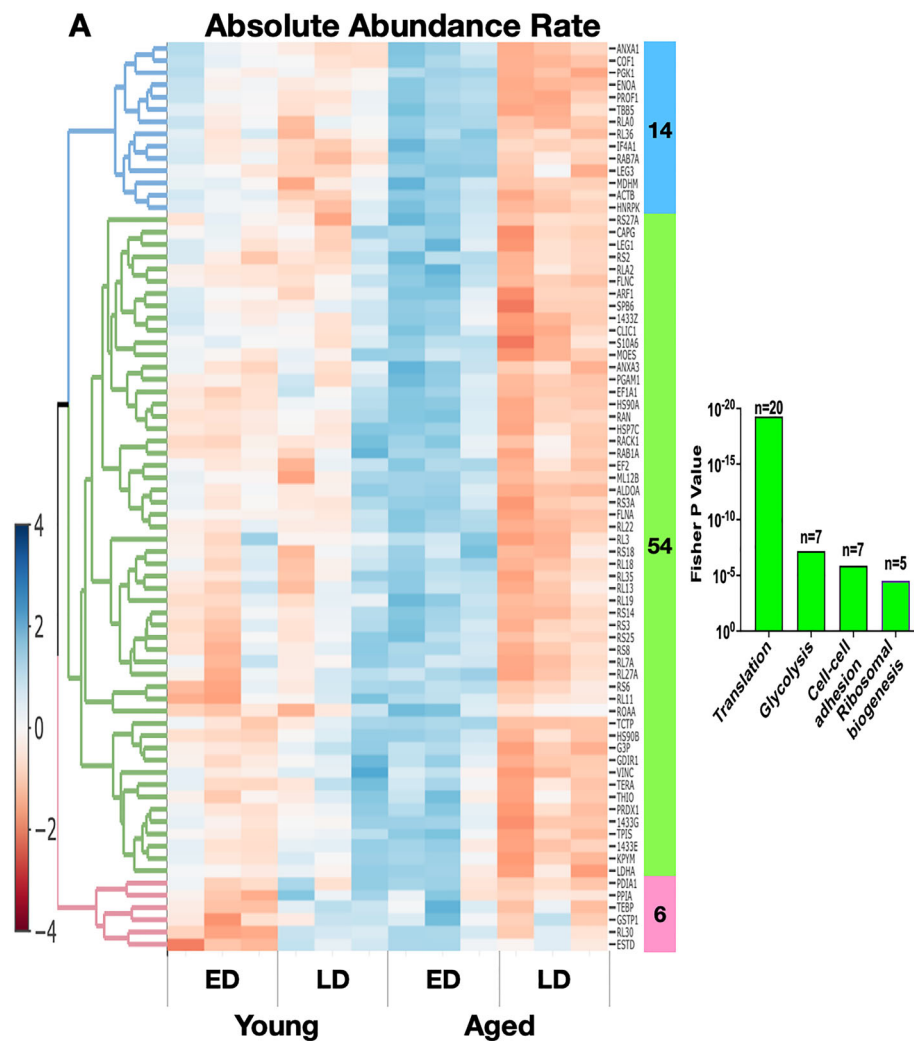


**Figure 3** Protein rate of abundance change in young and aged cells during early and later differentiation. Heatmap of proteins with significant interaction ( $P < 0.05$ ; FDR 5%) between age and early/late differentiation absolute abundance rates with 74 proteins. Blue increased and red decreased expression. Proteins were clustered based on dendrogram on left of heatmap and to the right of the heatmap, top-ranked biological processes of 54 proteins clustered in green displayed in bar graph. All experiments  $N = 3$  in duplicate.

differentiation period. The protein responses specific to aged cells encompassed several significantly (all Fisher  $P < 0.001$ ) enriched biological processes, including translation, glycolysis, cell–cell adhesion and ribosomal biogenesis. In aged myoblasts several proteins associated with translation initiation and elongation (eukaryotic initiation factor 4A-I, IF4A1; elongation factor 1- $\alpha$  1, EF1A1; and elongation factor 2, EF2) exhibited significantly greater ABR than young cells, which rescued the abundance to the level of the young. In addition, 18 ribosomal proteins (10 large ribosomal subunits and 8 small ribosomal subunits) exhibited greater gains in abundance during early compared with late differentiation in aged cells. Three chaperone proteins (heat shock protein 90  $\alpha$ ; HS90A, heat shock protein 90  $\beta$ , HS90B, heat shock cognate 71 kDa protein; HSP7C) also displayed greater gains in

abundance during early compared with late differentiation in aged cells and similar significant patterns of change were evident in the abundance of enzymes involved in glycolytic energy metabolism and cell adhesion. Proteins associated with myofibrillogenesis, including myosin-3,  $\alpha$  actin and desmin were included in our analysis but did not exhibit significant differences in ABR between young and aged cells during either early or later periods of differentiation.

Two-way ANOVA of the absolute abundance (ABD), synthesis rate (ASR) and degradation rate (ADR) was used to investigate differences between young and aged cells from the onset (0 h) to the end (24 h) of the early differentiation process (Figure 4). Thirty-nine proteins exhibited significant ( $P < 0.05$ ; FDR 5%) interactions in ABD between age and time (Figure 4A), and the biological processes enriched (Fisher

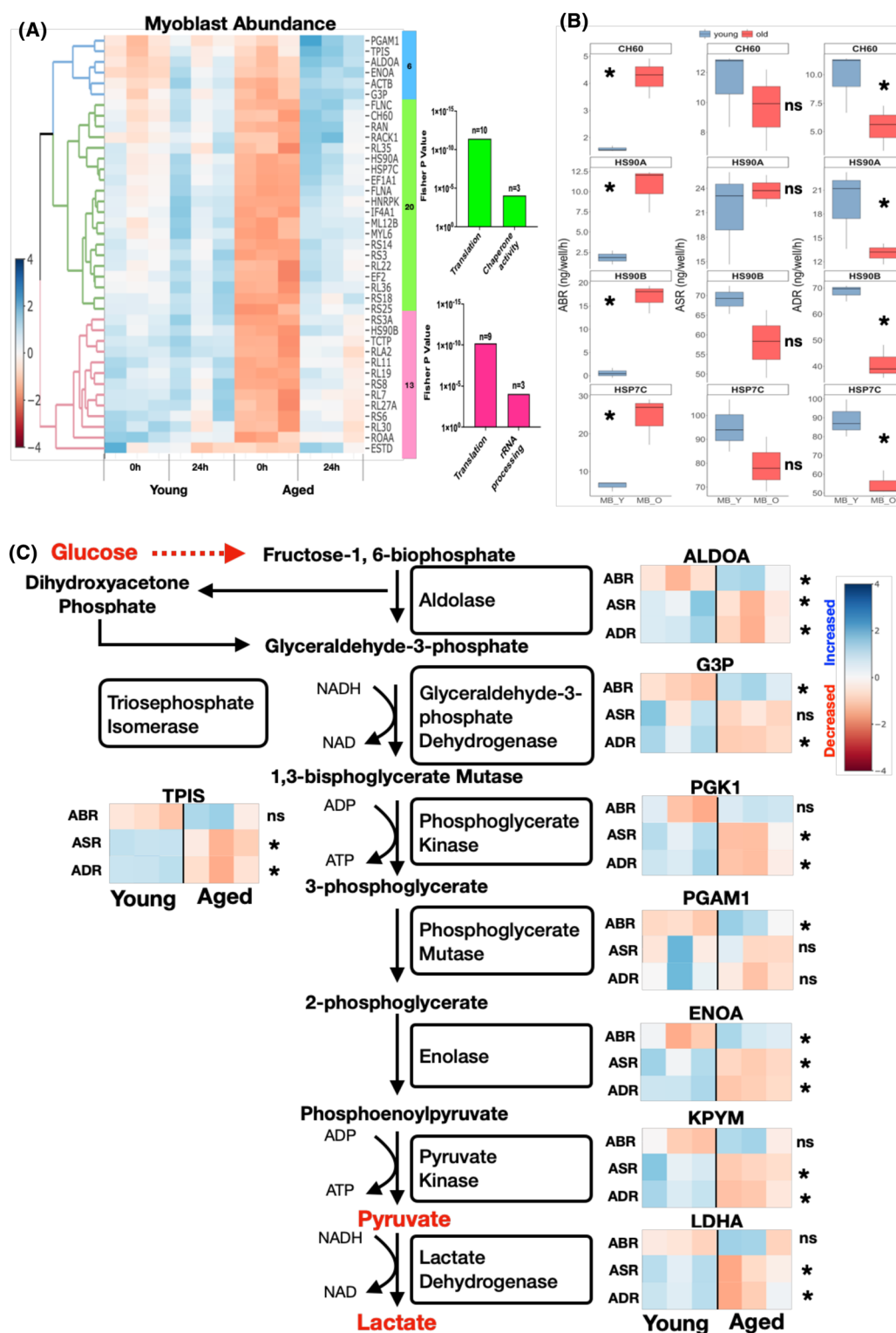


**Figure 4** Proteo-ADPT in young and replicatively aged cells during early differentiation. (A) Heatmap of proteins with significant interaction ( $P < 0.05$ ; FDR 5%) between age and cell absolute abundance with 49 proteins. Blue increased and red decreased expression. Proteins were clustered based on dendrogram on left of heatmap and to the right of the heatmap, top-ranked biological processes were displayed in bar graphs with corresponding number of proteins. (B) Selected individual protein rate of abundance change, absolute synthesis and degradation rates in young and aged myoblasts. (C) Proteo-ADPT model on enzymes identified in glycolysis pathway. Significance between young and aged indicated with \*. All experiments  $N = 3$  in duplicate.

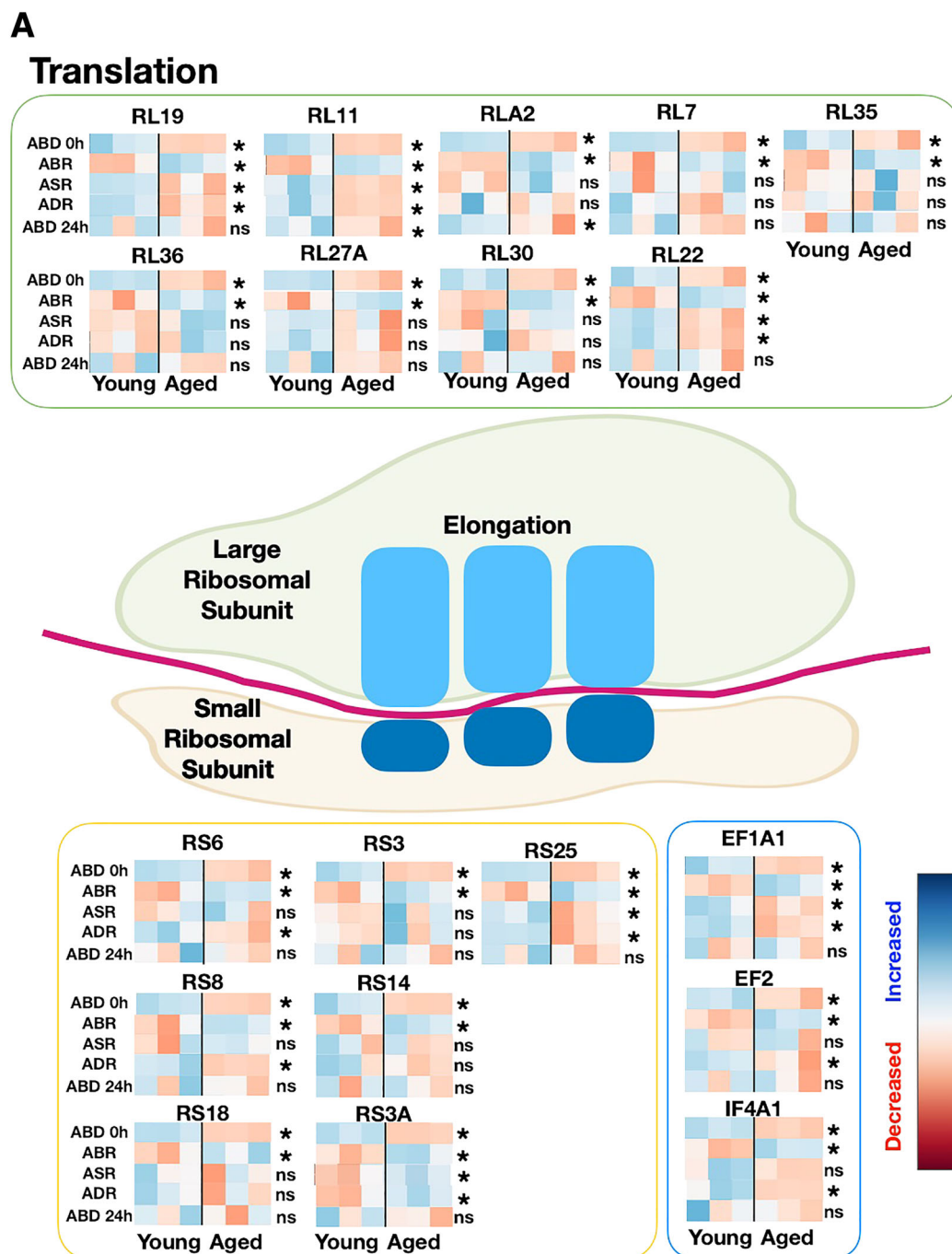


**Figure 5** Proteo-ADPT of translation proteins between young and replicatively aged cells during early differentiation. Absolute abundance and Proteo-ADPT data on ribosomal proteins identified in the current analysis. Blue increased and red decreased expression. Significance between young and aged indicated with \*. All experiments  $N = 3$  in duplicate.

$P < 0.001$ ) amongst these proteins included chaperone activity, glycolysis and translation. At the beginning of the labelling period the chaperone proteins HS90A, HS90B, HSP7C and 60 kDa heat shock protein (CH60) were significantly more abundant in young compared with aged cells but this difference was not evident at the end of the labelling period

(Figure 4A). The synthesis rates of the chaperone proteins were similar in young and aged cells and the greater rate of increase in abundance was due to significantly lesser degradation of the chaperone proteins in aged cells. For example, the abundance of HS90A increased at a rate of  $10.62 \pm 1.60$  ng/well/h in aged which was significantly greater



than  $1.86 \pm 0.49$  ng/well/h in young cells (Figure 4B). The ASR in young ( $21.23 \pm 3.40$  ng/well/h) versus aged ( $23.69 \pm 1.13$  ng/well/h) were equivalent and the ADR was significantly ( $P = 0.05$ ) greater in young compared with aged cells ( $19.37 \pm 2.93$  ng/well/h vs.  $13.06 \pm 0.76$  ng/well/h).

The abundance of several glycolytic enzymes was also less in aged than young cells at the beginning of the labelling period and, similar to the chaperone proteins, these differences in abundance were recovered in aged cells by the 24 h time point. Unlike chaperone proteins, however, age-related differences in the abundance changes of glycolytic enzymes were not entirely explained by differences in degradation rates. Eight glycolytic enzymes exhibited significant differences between young and aged cells in either abundance (Figure 4A), synthesis and/or degradation rates (Figure 4C). For example, the greater rate of increase in fructose-bisphosphate aldolase A (ALDOA) and alpha-enolase (ENOA) in aged cells was driven by greater synthesis rates (Figure 4C; Table S1). Conversely, the greater gain in abundance of glyceraldehyde-3-phosphate dehydrogenase (G3P) in aged cells was due to a lower degradation rate of G3P in aged compared with young cells. Triosephosphate isomerase (TPIS), phosphoglycerate kinase 1 (PGK1), pyruvate kinase (KPYM) and L-lactate dehydrogenase A chain (LDHA) exhibited no difference in ABR between young and aged cells but the turnover of these proteins was significantly greater in young myoblasts (Figure 4C; Table S1).

At the onset of differentiation, young myoblasts had a significantly greater abundance of 19 ribosomal proteins (Figure 5A; Table S2), and the abundance of ribosomal proteins remained stable throughout the early differentiation period. In aged cells the abundance of ribosomal proteins increased during early differentiation so that by 24 h, only two proteins (60S ribosomal protein L11; RL11 and 60S acidic ribosomal protein P2; RLA2) remained significantly more abundant in young myoblasts. The majority (13 of 19 proteins) of changes in protein abundance were not explained by heightened synthesis in aged cells. Indeed, EF1A1, RL11, 60S ribosomal protein L19 (RL19), 60S ribosomal protein L22 (RL22) and 40S ribosomal protein S25 (RS25) exhibited greater ASR in young cells but the gain in the abundance of these proteins was greater in aged cells. Accordingly, the degradation rates of RL11, 40S ribosomal protein S6 (RS6), 40S ribosomal protein S8 (RS8), RL19, RL22, EF2, EF1A1, IF4A1, and RS25 were significantly less in aged cells and accounted for the greater gains in the abundance of these proteins. Only RL11 had significantly greater abundance and turnover in young cells, whereas 40S ribosomal protein S3A (RS3A) had significantly greater turnover in aged cells. Five proteins (EF1A1, RL11, RL19, RL22, and RS25) had significantly greater turnover in young compared with aged cells and did not exhibit differences in protein abundance (i.e. abundance was at equilibrium between 0 and 24 h of differentiation).

During the later period (72–96 h) of differentiation, the abundance of six proteins [KPYM, HS90A, HS90B, filamin-A (FLNA), EF1A1, and 6-phosphogluconate dehydrogenase (6PGD)] exhibited a statistical interaction ( $P < 0.05$ ; FDR 5%) between time and age (Figure 6A). Generally, these proteins were significantly less abundant in aged compared with young cells at the 72 h time point and further reduced in abundance specifically in aged cells during the 72 to 96 h period.

In young cells the abundance of HS90A increased (positive ABR of  $6.65 \pm 1.51$  ng/well/h; Figure 6B) underpinned by a positive net balance between synthesis and degradation (ASR =  $28.14 \pm 3.70$  ng/well/h vs. ADR =  $21.49 \pm 3.13$  ng/well/h). Conversely, in aged cells, the degradation rate of HS90A ( $8.94 \pm 0.38$  ng/well/h) outweighed the rate of synthesis ( $7.89 \pm 1.28$  ng/well/h) meaning that the turnover of HS90A was also significantly less compared with young cells. Similarly, HS90B abundance increased at a rate of  $12.63 \pm 3.76$  ng/well/h, in young cells which was significantly different ( $P < 0.05$ ) from the rate of loss ( $-1.47 \pm 2.07$  ng/well/h) in abundance of HS90B in aged cells (Figure 6C). In young cells, HS90B was synthesized at a rate of  $61.98 \pm 2.57$  ng/well/h and degraded at a rate of  $49.35 \pm 6.17$  ng/well/h. In aged cells, HS90B rates of synthesis ( $22.46 \pm 2.51$  ng/well/h) and degradation ( $23.93 \pm 2.13$  ng/well/h) were lower compared with young cells and balanced in favour of a reduction in HS90B protein abundance. FLNA abundance gain was  $20.89 \pm 7.84$  ng/well/h in young cells; whereas in aged cells, the abundance rate decreased at  $-7.03 \pm 2.39$  ng/well/h (Figure 6C). Similar to the heat shock proteins, HS90A and HS90B, the contrasting abundance change in FLNA was a result of greater synthesis than degradation in young (ASR =  $133.87 \pm 17.68$  vs. ADR =  $112.98 \pm 25.20$  ng/well/h) compared with greater degradation than synthesis in aged (ASR =  $30.70 \pm 3.51$  ng/well/h vs. ADR =  $31.08 \pm 3.46$  ng/well/h). In contrast to the patterns of the aforementioned proteins, the abundance of 6PGD decreased in young and increased in aged cells during the late differentiation period (Figure 6B). That is, 6PGD displayed a negative rate of abundance change of  $-0.37 \pm 0.03$  ng/well/h in young and a positive rate of change  $0.67 \pm 0.23$  ng/well/h in aged (Figure 6C). The decline in 6PGD abundance was driven by greater degradation than synthesis in young (ASR =  $2.62 \pm 0.51$  ng/well/h vs. ADR =  $2.99 \pm 0.53$  ng/well/h), whereas synthesis was greater than degradation in aged cells (ASR =  $1.30 \pm 0.34$  ng/well/h vs. ADR =  $0.63 \pm 0.22$  ng/well/h).

## Discussion

Repair and regeneration of myofibres may be diminished or inefficient in aged compared with young muscle. We used

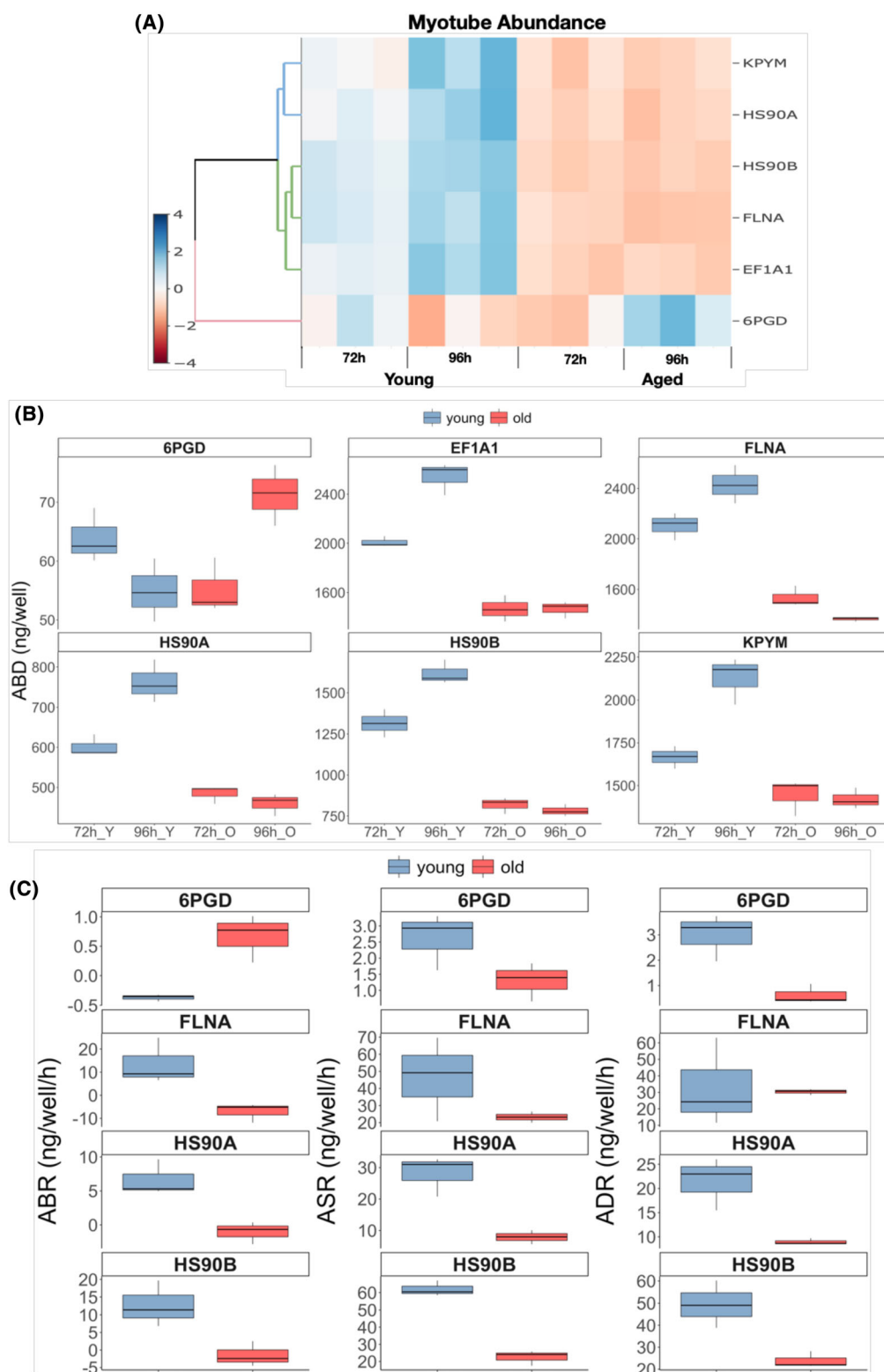


**Figure 6** Proteo-ADPT in young and replicatively aged cells throughout later differentiation. (A) Heatmap of proteins with significant interaction ( $P < 0.05$ ; FDR 5%) between age and cell absolute abundance with six proteins. Blue increased and red decreased expression. Proteins were clustered based on dendrogram on left of heatmap. (B) Individual proteins ABD in young and aged myoblasts at late differentiation. (C) Selected individual protein rate of abundance change, absolute synthesis and degradation rates in young and aged myoblasts at late differentiation. All experiments  $N = 3$  in duplicate.

Proteo-ADPT<sup>21</sup> to investigate the absolute abundance, synthesis, and degradation rates of individual proteins in low passage young and replicatively-aged myoblasts during early and late periods of differentiation. Young cells exhibited a steady pattern of growth, protein accretion and fusion throughout the first 96 h of differentiation. In contrast, aged myoblasts exhibited markedly different proteome responses during early differentiation and failed to gain protein mass or undergo fusion during later differentiation (Figure 7). Our novel Proteo-ADPT data provide new evidence suggesting that the maturation of the proteome may be retarded in aged myoblasts at the onset of differentiation but quickly catches up with the young cells during the first 24 h period. However, this 'catch up' process in aged cells is not accomplished by higher levels of protein synthesis. Instead, a lower level of protein degradation in aged cells was responsible for the gains in protein abundance. As differentiation progressed, aged cells also did not fuse into myotubes and their protein content declined. Our novel data point to a loss of quality of key proteins as a precursor to the lack of fusion of aged myoblasts and highlights dysregulation of protein degradation, particularly of ribosomal and chaperone proteins, as a key mechanism that may contribute to age-related declines in the capacity of myoblasts to undergo differentiation.

Chaperone proteins are integral to proteostasis and regulate myoblast differentiation by interacting with key cell signalling pathways.<sup>22</sup> Substrate proteins or targets of the alpha (HS90A) and beta (HS90B) isoforms of heat shock protein 90 (HSP90) include regulatory factors, such as MyoD and myogenin (key myogenic regulatory proteins), and Akt, all of which are required for myogenic differentiation.<sup>22</sup> We discovered that aged myoblasts had a significantly lower abundance of HS90A and HS90B at the onset of differentiation, and although the abundance of HS90A and HS90B recovered to levels equivalent to young cells after 24 h of differentiation, this accelerated gain in abundance was not achieved by a rise in the synthesis rate of HS90A or HS90B. Instead, a lack of degradation of HSP90 isoforms in aged cells was associated with the accumulation in protein abundance during early differentiation, which may suggest the quality of these chaperone proteins in aged cells was suboptimal at the 24 h time point. During later differentiation, the abundance of HS90A and HS90B was reduced in aged cells that failed to undergo fusion and form myotubes, unlike in young cells, which exhibited significant protein accretion and successfully formed myotubes. Inhibition of HSP90 retards muscle regeneration *in vivo* and stalls protein accretion and the fusion of myoblasts in to myotubes *in vitro*<sup>22</sup> in a manner that closely resembles our findings in replicatively aged myoblasts. FLNA acts as a mechanotransducer during cell migration and differentiation and during cell alignment, which precedes fusion, filamins rapidly unfold and dictate movement at the leading cell edge<sup>23</sup> and this unfolding is driven by binding to HSP90.<sup>24</sup> Therefore, our data suggest the age-related reduc-

tion in FLNA and HSP90 abundance could be associated with the lack of fusion during later differentiation.

Heat shock protein 70 (HSP70) and CH60 work cooperatively with HSP90,<sup>24</sup> and we report HSP7C and CH60 exhibit age-dependent differences in protein abundance, synthesis and degradation similar to the patterns exhibited by HS90A and HS90B (Figure 4B). Diminished expression of either the inducible 70 kDa heat shock protein (HSPA1) or the closely related HSP7C disrupts differentiation of C2C12 myoblasts<sup>25</sup> similar to the effects HSP90 inhibition,<sup>22</sup> however the interacting proteins and kinase pathways involved are likely to be different. While HSP90 impacts Akt-related signalling, the MAPK p38 $\alpha$  is the key client of the HSP70 proteins.<sup>25</sup> P38 MAPK interacts with the transcription factors MEF2 and MyoD to regulate myoblast differentiation<sup>26</sup> and HSP70 and is required for myoblast differentiation *in vitro* and muscle regeneration *in vivo*.<sup>25</sup> Loss of HSP70 can be rescued by either enhancing p38 MAPK or through proteasome inhibition,<sup>25</sup> which implies that HSP70 stabilizes and prevents the degradation of p38 MAPK. CH60 is a key mitochondrial chaperone in adult muscle but its role in myoblast differentiation is less explored, but warrants further investigation based on the current finding that CH60 exhibits similar responses to members of the 70 and 90 kDa heat shock protein families.

The enzyme, 6PGD, was unique in that it was the only protein amongst those investigated that exhibited a significant gain in abundance specifically in aged cells during the later period of differentiation. 6PGD is the rate limiting enzyme in the pentose phosphate pathway and catalyses the reaction between ribulose 5-phosphate and 6-phosphogluconate, which produces NADPH that may be associated with a heightened generation of reactive oxygen species (ROS).<sup>27</sup> In C2C12 myoblasts and myotubes, increased ROS via myostatin treatment upregulated the activity of NADPH oxidases via the translocation and activation of NF- $\kappa$ B to the nucleus.<sup>27</sup> Induction of ROS upregulated NF- $\kappa$ B signalling and acted as a feedforward loop to increase secretion of myostatin,<sup>27</sup> further accelerated the induction of these signalling pathways. However, based on the current data it is unclear whether the rise in 6PGD abundance further accelerates damage or, alternatively, represents a counter attempt to recover losses in proteostasis in aged cells. For example, elevated G6PD abundance could promote cell survival by protecting against elevated ROS production via activation of NF- $\kappa$ B. While NF- $\kappa$ B were not investigated in the current work, this response would be expected to lead to lesser expression of MyoD.<sup>9</sup> In the same study, NF- $\kappa$ B inducing kinase (NIK) directly phosphorylated G6PD and over-expression of NIK subsequently elevated G6PD. Therefore, elevated G6PD could act to protect cells from excessive ROS production (potentially activated by elevated myostatin) through elevated NF- $\kappa$ B and NIK. Consequently, elevated NF- $\kappa$ B could suppress MyoD which was reported in replicatively aged cells.<sup>9</sup>

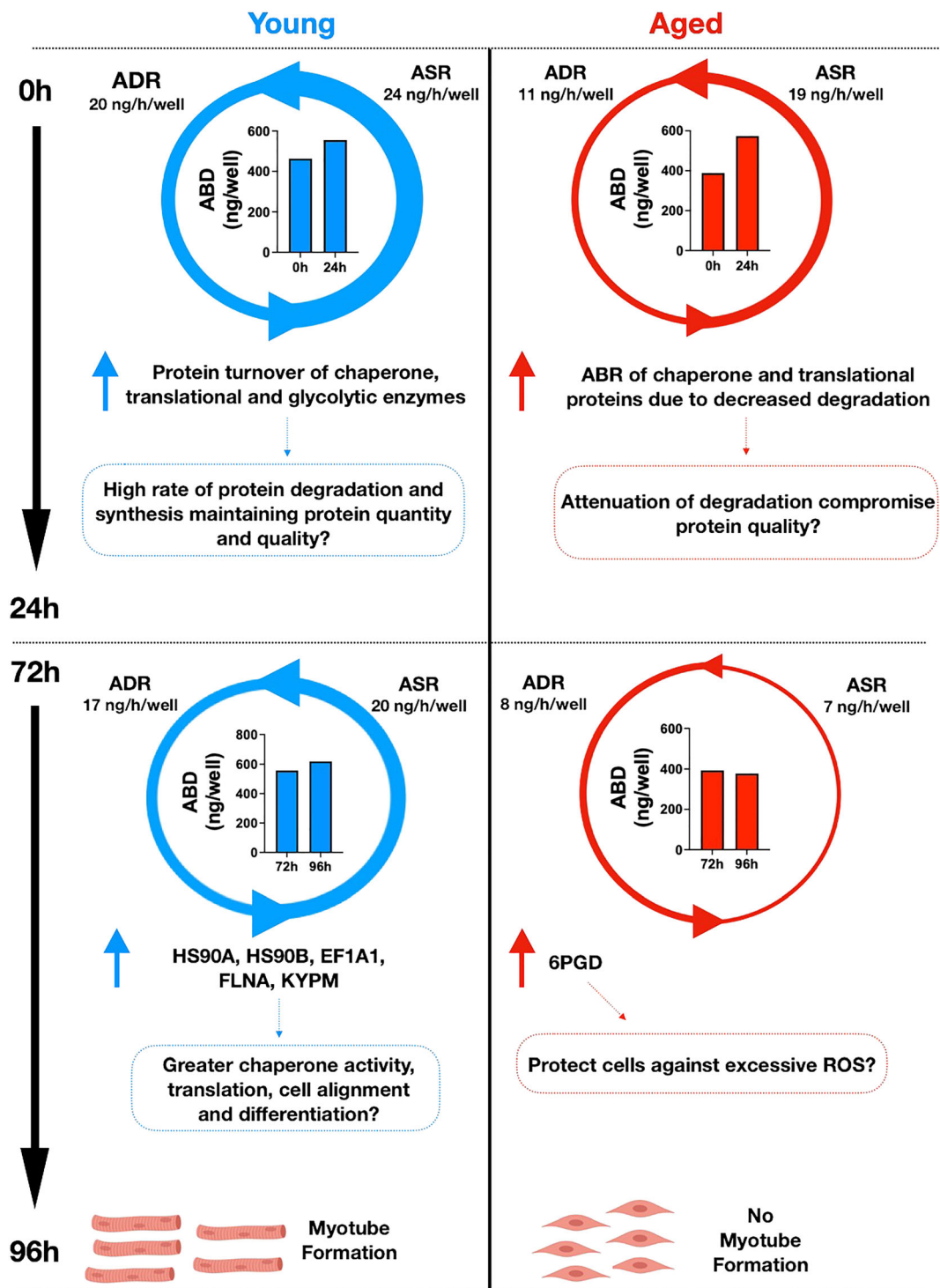


**Figure 7** Summary of young compared with replicatively aged cells during early and late myoblast differentiation. The summary of our findings on young myoblasts are on the left column and aged on the right column. Downwards arrows covers early and late myoblast differentiation. Size of circular arrows corresponds to degradation and synthesis rates. HS90A, heat shock protein 90 alpha; HS90B, heat shock protein 90 beta; EF1A1, elongation factor 1-alpha 1; FLNA, filamin-a; KYPM, pyruvate kinase; 6PGD, 6-phosphogluconate dehydrogenase; ROS, reactive oxygen species.

Glycolysis is the dominant energy source in proliferating myoblasts and upon differentiation there is a gradual transition to a greater contribution of ATP resynthesis by oxidative phosphorylation.<sup>28</sup> Seven out of eight enzymes of glycolytic metabolism exhibited significant disruption in either abundance or turnover in aged compared with young cells. Proteo-ADPT data for glycolytic enzymes were markedly different to the patterns exhibited by ribosomal and chaperone proteins. In young cells, there was a general decline in the abundance of glycolytic enzymes, which is consistent with our earlier findings and the greater energy requirements associated with higher levels of protein synthesis in myoblasts compared with myotubes.<sup>13</sup> In aged myoblasts, four glycolytic proteins exhibited increased abundance and the turnover of seven glycolytic enzymes was impaired in aged compared with young myoblasts during early differentiation. Dysfunction of glycolytic energy metabolism is associated with an accelerated onset of brain ageing.<sup>29</sup> For instance, TPIS, the mid-point catalyst between hexose and triose stages of glycolysis, exhibited impaired turnover and no difference in the rate of abundance change in aged compared with young myoblasts. In support, TPIS protein content was impaired in the aged brain and consequently, there was reduced NADH metabolism and an increase in the bioproduct methylglyoxal which activates advanced glycation end-products.<sup>29</sup>

Our findings point to age effect on UPS or other degradation processes, but protein subunits of UPS and autophagy were not specifically identified within the current analyses. Further work using higher resolution MS is warranted in this model of muscle ageing. In *C elegans* turnover and abundance of proteasome subunits is maintained during ageing but muscle proteins are not particularly enriched in whole worms. Ubiquitinated proteins accumulate in liver of aged mice<sup>30</sup> suggesting impaired degradation occurred earlier in life supporting the role of UPS in healthy ageing. C2C12 cells exhibit little or no proliferation upon transfer to differentiation medium,<sup>13</sup> which enables protein synthesis rates to be calculated against a consistent background, but future studies

should also investigate the effects of ageing in proliferating myoblasts before the transition to differentiation media. In addition, our analyses highlight the mid-differentiation period (24–72 h) as a key time where differences in fusion occur and Proteo-ADPT analysis including this timespan may shed new light on the mechanisms that specifically impair the fusion of replicatively aged myoblasts.

In conclusion, replicatively aged myoblasts exhibit significant disruption in the normal proteome dynamics associated with differentiation in young cells (*Figure 7*). In particular, our data suggest the quality of key chaperone proteins, including HS90A, HS90B and HSP7C was reduced in aged cells and may account for the disruption to cell signalling required for differentiation and fusion. Our findings and the associated literature suggest a failure in protein degradation may cause disruption to ribosomal capacity that subsequently impairs protein synthesis, and thus muscle homeostasis and health.

## Acknowledgements

Authors would like to thank Liverpool John Moores University for providing funding for the project. The authors of this manuscript certify that they comply with the ethical guidelines for authorship and publishing in the *Journal of Cachexia, Sarcopenia and Muscle*.<sup>31</sup>

## Conflict of interest

The authors declare no conflicts of interest.

## Online supplementary material

Additional supporting information may be found online in the Supporting Information section at the end of the article.

## References

1. Collins CA, Olsen I, Zammit PS, Heslop L, Petrie A, Partridge TA, et al. Stem cell function, self-renewal, and behavioral heterogeneity of cells from the adult muscle satellite cell niche. *Cell* 2005;**122**: 289–301.
2. Conboy IM, Rando TA. Aging, stem cells and tissue regeneration: lessons from muscle. *Cell Cycle* 2005;**4**:407–410.
3. Verdijk LB, Snijders T, Drost M, Delhaas T, Kadi F, van Loon LJC. Satellite cells in human skeletal muscle; from birth to old age. *Age* 2014;**36**:545–557.
4. Brack AS, Rando TA. Intrinsic changes and extrinsic influences of myogenic stem cell function during aging. *Stem Cell Rev* 2007; **3**:226–237.
5. Lees SJ, Rathbone CR, Booth FW. Age-associated decrease in muscle precursor cell differentiation. *Am J Physiol Cell Physiol* 2006;**290**:C609–C615.
6. Lorenzon P, Bandi E, de Guarrini F, Pietrangelo T, Schäfer R, Zweyer M, et al. Ageing affects the differentiation potential of human myoblasts. *Exp Gerontol* 2004; **39**:1545–1554.
7. Alsharidah M, Lazarus NR, George TE, Agley CC, Velloso CP, Harridge SDR. Primary human muscle precursor cells obtained from young and old donors produce similar proliferative, differentiation and senescent profiles in culture. *Aging Cell* 2013;**12**: 333–344.
8. Bigot A, Jacquemin V, Debacq-Chainiaux F, Butler-Browne GS, Toussaint O, Furling D, et al. Replicative aging down-regulates the myogenic regulatory factors in human myoblasts. *Biol Cell* 2008;**100**:189–199.



9. Sharples AP, Al-Shanti N, Lewis MP, Stewart CE. Reduction of myoblast differentiation following multiple population doublings in mouse C2C12 cells: a model to investigate ageing? *J Cell Biochem* 2011;**112**:3773–3785.
10. Moustogiannis A, Philippou A, Taso O, Zevolis E, Pappa M, Chatzigeorgiou A, et al. The Effects of Muscle Cell Aging on Myogenesis. *Int J Mol Sci* 2021;**22**:3721.
11. Brown AD, Close GL, Sharples AP, Stewart CE. Murine myoblast migration: influence of replicative ageing and nutrition. *Biogerontology* 2017;**18**:947–964.
12. Nozaki T, Nikai S, Okabe R, Nagahama K, Eto N. A novel in vitro model of sarcopenia using BubR1 hypomorphic C2C12 myoblasts. *Cytotechnology* 2016;**68**:1705–1715.
13. Stansfield BN, Brown AD, Stewart CE, Burniston JG. Dynamic Profiling of Protein Mole Synthesis Rates During C2C12 Myoblast Differentiation. *Proteomics* 2020;2000071.
14. Ubaida-Mohien C, Lyashkov A, Gonzalez-Freire M, Tharakan R, Shardell M, Moaddel R, et al. Discovery proteomics in aging human skeletal muscle finds change in spliceosome, immunity, proteostasis and mitochondria. *Elife* 2019;**8**:e49874.
15. Fernando R, Drescher C, Nowotny K, Grune T, Castro JP. Impaired proteostasis during skeletal muscle aging. *Free Radic Biol Med* 2019;**132**:58–66.
16. Santra M, Dill KA, de Graff AM. Proteostasis collapse is a driver of cell aging and death. *Proc Natl Acad Sci* 2019;**116**:22173–22178.
17. Chondrogianni N, Georgila K, Kourtis N, Tavernarakis N, Gonos ES. 20S proteasome activation promotes life span extension and resistance to proteotoxicity in *Caenorhabditis elegans*. *FASEB J* 2015;**29**:611–622.
18. Burniston JG. Investigating Muscle Protein Turnover on a Protein-by-Protein Basis Using Dynamic Proteome Profiling. In *Omics Approaches to Understanding Muscle Biology*. New York, NY: Springer; 2019. p 171–190. [https://doi.org/10.1007/978-1-4939-9802-9\\_9](https://doi.org/10.1007/978-1-4939-9802-9_9)
19. Gerner C, Vejda S, Gelbmann D, Bayer E, Gotzmann J, Schulte-Hermann R, et al. Concomitant determination of absolute values of cellular protein amounts, synthesis rates, and turnover rates by quantitative proteome profiling. *Mol Cell Proteomics* 2002;**1**:528–537.
20. Kristensen AR, Gsponer J, Foster LJ. Protein synthesis rate is the predominant regulator of protein expression during differentiation. *Mol Syst Biol* 2013;**9**:689.
21. Hesketh SJ, Sutherland H, Lisboa PJ, Jarvis JC, Burniston JG. Adaptation of rat fast-twitch muscle to endurance activity is underpinned by changes to protein degradation as well as protein synthesis. *FASEB J* 2020;**34**:10398–10417.
22. Wagatsuma A, Shiozuka M, Kotake N, Takayuki K, Yusuke H, Mabuchi K, et al. Pharmacological inhibition of HSP90 activity negatively modulates myogenic differentiation and cell survival in C2C12 cells. *Mol Cell Biochem* 2011;**358**:265–280.
23. Nakamura F, Song M, Hartwig JH, Stossel TP. Documentation and localization of force-mediated filamin A domain perturbations in moving cells. *Nat Commun* 2014;**5**:1–11.
24. Schneider C, Sepp-Lorenzino L, Nimmesgern E, Ouerfelli O, Danishefsky S, Rosen N, et al. Pharmacologic shifting of a balance between protein refolding and degradation mediated by Hsp90. *Proc Natl Acad Sci* 1996;**93**:14536–14541.
25. Fan W, Gao XK, Rao XS, Shi YP, Liu XC, Wang FY, et al. Hsp70 interacts with mitogen-activated protein kinase (MAPK)-activated protein kinase 2 to regulate p38MAPK stability and myoblast differentiation during skeletal muscle regeneration. *Mol Cell Biol* 2018;**38**. <https://doi.org/10.1128/MCB.00211-18>
26. Brennan CM, Emerson CP, Owens J, Christoforou N. p38 MAPKs—roles in skeletal muscle physiology, disease mechanisms, and as potential therapeutic targets. *JCI insight* 2021;**6**. <https://doi.org/10.1172/jci.insight.149915>
27. Sriram S, Subramanian S, Sathiakumar D, Venkatesh R, Salerno MS, McFarlane CD, et al. Modulation of reactive oxygen species in skeletal muscle by myostatin is mediated through NF- $\kappa$ B. *Aging Cell* 2011;**10**:931–948.
28. Relaix F, Bencze M, Borok MJ, der Vartanian A, Gattazzo F, Mademtzoglou D, et al. Perspectives on skeletal muscle stem cells. *Nat Commun* 2021;**12**:1–11.
29. Cai W, Uribarri J, Zhu L, Chen X, Swamy S, Zhao Z, et al. Oral glycotoxins are a modifiable cause of dementia and the metabolic syndrome in mice and humans. *Proc Natl Acad Sci* 2014;**111**:4940–4945.
30. Basisty NB, Liu Y, Reynolds J, Karunadharma PP, Dai DF, Fredrickson J, et al. Stable isotope labeling reveals novel insights into ubiquitin-mediated protein aggregation with age, calorie restriction, and rapamycin treatment. *J Gerontol Ser A* 2018;**73**:561–570.
31. von Haehling S, Morley JE, Coats AJS, Anker SD. Ethical guidelines for publishing in the Journal of Cachexia, Sarcopenia and Muscle: update 2021. *J Cachexia Sarcopenia Muscle* 2021;**12**:2259–2261.